Development Conditions for Tropical Storms
over the Western North Pacific Stratified by Large-Scale Flow Patterns

Hironori FUDEYASU

Yokohama National University, Yokohama, Japan

Ryuji YOSHIDA

CIRES, University of Colorado Boulder, Colorado, USA
NOAA Earth System Research Laboratory, Colorado, USA
RIKEN Center for Computational Science, Kobe, Japan
Research Center for Urban Safety and Security, Kobe University, Kobe, Japan

Munehiko YAMAGUCHI

Meteorological Research Institute, Tsukuba, Japan

**Hisaki EITO, Chiashi MUROI, Shuji NISHIMURA, Kotaro BESSHO,
Yoshinori OIKAWA, and Naohisa KOIDE**

Japan Meteorological Agency, Tokyo, Japan

Abstract

   This study investigated the characteristics and environmental conditions of tropical cyclones (TCs) over the western North Pacific from 2009 to 2017 that dissipated before reaching tropical storm strength (TDs) under unfavorable environmental conditions; we compared TDs with TCs that reached tropical storm strength (TSs) in terms of modulations of relevant large-scale flow patterns. The flow patterns were categorized based on five factors: shear line, confluence region, monsoon gyre, easterly waves, and Rossby wave energy dispersion from a preexisting cyclone. Among 476 cases, 263 TDs were detected using best-track data and early stage Dvorak analysis. The TCs in the environments associated with the confluence region or Rossby wave energy dispersion (easterly waves) tended to reach tropical storm strength (remain weak) compared with the other factors. The average locations of TDs at the time of cyclogenesis in the confluence region, monsoon gyre, and easterly waves (Rossby wave energy dispersion) in the summer and autumn were farther to the west (east and north) than those of TSs that exhibited the same factors. The environments around TDs were less favorable for development than those around TSs, as there were significant differences in atmospheric (oceanic) environmental parameters between TDs and TSs in the factors of confluence region, easterly waves, and Rossby wave energy dispersion (shear line, monsoon gyre, and Rossby wave energy dispersion). The environmental conditions for reaching tropical storm strength over their developing stage, using five factors, can be summarized as follows: higher tropical cyclone heat potential in the shear line and monsoon gyre, weak vertical shear in the confluence region, wet conditions in the easterly waves, and higher sea surface temperatures and an intense preexisting cyclone in Rossby wave

Corresponding author: Hironori Fudeyasu, Faculty of Education, Yokohama National University, 79-2 Tokiwadai, Hodogaya-ku, Yokohama, 240-8501, Japan
E-mail: fude@ynu.ac.jp

energy dispersion from a preexisting cyclone.

1.   Introduction

Tropical cyclones (TCs) form under the large-scale environmental conditions favorable for cyclogenesis (TCG) during their TCG stage. According to Gray (1968, 1998), the environmental conditions favorable for TCG include sea temperatures to a depth of 60 m that exceed 26°C and large-scale flow patterns. Ritchie and Holland (1999) grouped the lower-tropospheric large-scale atmospheric flow patterns contributing to TCG over the western North Pacific (WNP) into five factors: shear line (SL), confluence region (CR), monsoon gyre (GY), easterly waves (EW), and Rossby wave energy dispersion from a preexisting cyclone (PTC).

Some TCs during their developing stage may continue to strengthen, eventually reaching tropical storm strength, with maximum sustained wind speeds of 34 knots. However, some weaken and eventually dissipate before reaching tropical storm strength under unfavorable environmental conditions; in this study, the former are referred to as TSs and the latter as TDs. Although some previous studies (e.g., Zehr 1992; Peng et al. 2012; Fu et al. 2012; Zhang et al. 2015) have attempted to characterize differences in developing and non-developing tropical disturbances, none has addressed the favorable/unfavorable environmental conditions for TSs stratified by relevant large-scale flow patterns due to a lack of reliable TD data.

The Japan Meteorological Agency (JMA) developed a unique TC analysis technique, early stage Dvorak analysis (EDA), which has been in operation since 2001 (Tsuchiya et al. 2001; Kishimoto et al. 2007; Kishimoto 2008; Yamaguchi and Koide 2017). In a conventional Dvorak technique, a T number is assigned to a TC based on its strength; T numbers range from 1.0 to 8.0 at intervals of 0.5. In general, when TCs reach tropical storm strength, they are categorized as a T number of 2.5 (Koba et al. 1990; Dvorak 1984). In the EDA, the T numbers 0.0 and 0.5 are added to the conventional Dvorak technique to make it possible

to analyze TDs in their developing stage. Therefore, the operational EDA data list tracks for not only TSs but also TDs.

Although some weather prediction models are capable of detecting TS cases, there are still a lot of false alarm cases (Halperin et al. 2013, 2017; Yamaguchi et al. 2015). This study used operational EDA and reanalysis data to statistically investigate the unfavorable environmental conditions that result in maintaining TD status compared with those that lead to TS development, including both atmospheric and oceanic physical parameters. Large-scale flow patterns which contribute to TCG are expected during the development of a TD into a TS. Thus, the purpose of this study was to determine how different environmental factors contributing to TCG classified by Ritchie and Holland (1999) modulate the unfavorable environmental conditions resulting in TDs. The ability to identify these conditions would greatly facilitate forecasting operations (Blake and Kotal 2018; Yamaguchi et al. 2018).

This paper is organized as follows. Section 2 describes the data set and environmental physical parameters. Section 3 presents the statistical results depicting the characteristics and environmental conditions of TDs and TSs, as well as those stratified by five relevant environmental factors classified by Ritchie and Holland (1999). The favorable environmental conditions for TS development are discussed in Section 4. A summary and conclusions are presented in Section 5.

2.   Data and definitions

This study examined 476 TCs that occurred over the WNP during the 9 years from 2009 to 2017 from operational EDA data and best-track archive data of the Regional Specialized Meteorological Centers (RSMC) Tokyo–Typhoon Center (hereafter, best-track data). The EDA date added T numbers of 0.0 and 0.5 based on the following conditions: 1) a convective cloud system has persisted for 12 h or more; 2) the

cloud system, a cyclonic circulation, has a cloud system center defined within a diameter of 2.5° latitude or less; 3) the cloud system persisted for 6 h or more; 4) the cloud system has an area that is dense and cold (−31°C or colder) and that appears less than 2° latitude from the center; and 5) the above overcast is more than 1.5° latitude in diameter. A T number of 0.0 is assigned when three out of the five conditions are met, and a T number of 0.5 is assigned when four out of the five conditions are met. Details of the EDA algorithm were described in a recent study of Yamaguchi and Koide (2017).

TCs were categorized into TDs and TSs. Here, a TD refers to a TC listed in EDA data only; 213 TDs were revealed in the EDA data. Specifically, a TD is a TC detected by operational EDA that did not achieve tropical storm strength. A TS refers to a TC listed in both the EDA and best-track data; 263 TSs were identified from 476 TCs.

This study investigated the environmental physical parameters associated with TDs compared with those associated with TSs. The atmospheric parameters were calculated from the Japanese 55-year Reanalysis Project datasets (JRA55; Kobayashi et al. 2015) (details are available online at http://jra.kishou.go.jp/JRA-55/index_en.html), and the oceanic parameters were derived from the three-dimensional variational-based parent domain output from the Four-dimensional Variational Ocean Reanalysis for the WNP (FORA-WNP30) (Usui et al. 2017). The JRA55 reanalysis contains data collected at 6-h intervals with the horizontal resolution of 1.25° from 1958 to the present. FORA-WNP30 contains data at 6-h intervals with the horizontal resolution of 0.5° from 1982 to 2016, with 54 vertical levels from 0.5 to 6000 m in depth.

We evaluated the following atmospheric and oceanic physical parameters: upper-tropospheric divergence at 200 hPa (DIV200); lower-tropospheric relative vorticity at 850 hPa (VOR850); vertical shear defined as the difference in horizontal winds between 200 and 850 hPa (SHRD) and between 500 and 850 hPa (SHRS); lower- and middle-tropospheric relative humidity calculated over 850–700 hPa (RHLO) and 500–300 hPa (RHHI); maximum potential intensity (MPI) (Emanuel 1986, Bister and Emanuel 1998); convective available potential energy (CAPE) derived from the MPI equation; sea surface temperature (SST); tropical cyclone heat potential (TCHP); and depth of the 26°C oceanic isotherm. The TCHP was calculated by summing the ocean heat content from the sea surface to the depth of the 26°C isotherm (Leipper and Volgenau 1972; Wada 2015). The SST, TCHP, 26°C

oceanic isotherm, CAPE, and MPI were evaluated from 2009 to 2016, the period that coincided with FORA-WNP30. Two area averages were used in this study, similar to the approaches taken in several previous studies (e.g., Knaff et al. 2005): 1) the average for the circular area with an 800-km radius from the location of TCG and 2) an annulus of 200–800 km from the location of cyclone center. The former was used to evaluate oceanic physical parameters, and the latter was applied to the atmospheric physical parameters.

This study enhanced the statistical analysis of the characteristics and environmental conditions of TDs by examining modulation by five relevant environmental factors which contributed to TCG, namely, SL, CR, GY, EW, and PTC (Ritchie and Holland 1999). To categorize the five environmental factors, we used the TCG score detection method (TGS) developed by Yoshida and Ishikawa (2013) based on EDA and JRA55 data. The location and time of the first entry of EDA data were used as the TCG location and time. When the major environmental factors could not be found by the TGS, the flow pattern was categorized as unclassified flow (UCF). Details of the TGS algorithm are presented in Appendix A.

3.   Results

3.1   Characteristics and environmental conditions of TDs and TSs

Among the 476 TCs over the analysis period from 2009 to 2017, 263 TDs and 213 TSs were revealed. The occurrence rate of TDs, the number of TD divided by the total number of TCs, was 55 %, which is a higher rate than that of TSs. Figure 1a presents the average number of TDs and TSs for each month. TSs tended to occur in the summer and autumn, whereas TDs occurred throughout the year. Because this seasonal variation was due to seasonal variation in all TC occurrences, we divided the number of TDs and TSs by the monthly total of TCs, as presented in Fig. 1b. The TD occurrence rate was higher than that of TSs in the winter and spring, whereas the trend was completely opposite for the period from May to October.

Table 1 presents the average locations of TDs and TSs between June and October, typically a period during which many TDs and TSs may occur at almost the same monthly occurrence rate. Differences in the parameters between TDs and TSs were assessed using t-test. The average location of TDs at the time of TCG was farther to the west and north than that of TSs with a 5 % level of significance. Tracks of TDs and TSs, presented in Fig. 2, start at the TCG location, i.e., the locations of the first entry of EDA for each case.
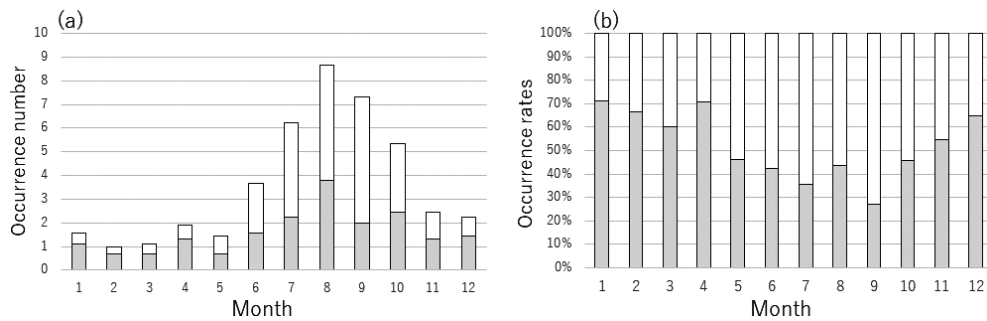
Fig. 1.   Seasonal variation in tropical depression (TD) and tropical storm (TS) occurrence over the 9-year analysis period: (a) monthly average numbers of TDs and TSs and (b) monthly occurrence rates normalized by the monthly total. Gray bars indicate TDs, and white bars indicate TSs.

Table 1.   Statistical summary of the tropical depressions (TDs) and tropical storms (TSs) associated with the environmental factors over a 9-year analysis period between June and October. The speed of TC movements is defined from the change of latitude and longitude, but it is different from the actual speed. Areas for which a *t*-test indicated differences at a 5 % level of significance are presented in bold and italic fonts, except for the number and duration. Note: average of all TCs, ALL; shear line, SL; confluence region, CR; monsoon gyre, GY; easterly waves, EW; Rossby wave energy dispersion, PTC; and unclassified flow, UCF.

	ALL		SL		CR		GY	
	TD	TS	TD	TS	TD	TS	TD	TS
Number	158	173	41	46	40	46	23	23
Ave. lon. (°E)	**138.61**	**142.31**	134.86	138.63	**134.37**	**139.15**	**131.91**	**140.99**
Ave. lat. (°N)	**15.36**	**14.40**	15.23	15.01	14.60	14.52	14.29	14.36
Speed (°day^{-1})	**3.16**	**2.85**	3.07	2.77	**3.44**	**2.47**	2.58	2.98
Duration (day)	1.39	1.21	1.49	1.09	1.24	1.24	1.62	1.15

	EW		PTC		UCF	
	TD	TS	TD	TS	TD	TS
Number	29	24	14	23	11	11
Ave. lon. (°E)	**141.79**	**149.43**	**162.52**	**153.67**	143.24	134.36
Ave. lat. (°N)	16.30	15.01	**13.44**	**11.19**	20.79	16.78
Speed (°day^{-1})	3.31	2.91	3.42	3.48	3.04	2.67
Duration (day)	1.11	1.66	1.93	1.07	1.14	1.00

The TCG locations of TSs were concentrated along 10−20°N longitude.

The statistical characteristics of TC movements were also investigated in this study. The speed of TC movements at the time of TCG was defined from the change in the location from the time of TCG to 1 day later. Note that TDs which had a lifetime of less than 1 day were excluded for the average of TC movements. The average speed of the movement of TDs and TSs at the time of TCG differed significantly, with TDs tending to move faster than TSs (Table 1).

Figure 3 presents the distribution of TD durations between the first and the final EDA entry for each TD between June and October over the analysis period. A TD duration of 6−12 h was the most common duration (30 %) observed, followed by the 18−24-h duration (25 %). Thus, over half of all TDs had a duration of less than 24 h, and the occurrence rates of TDs decreased as the duration increased. The average TD duration was 1.39 days (Table 1).

Tables 2 and 3 present the average atmospheric and oceanic environmental parameters for TDs and TSs at the time of TCG. There were significant differences in the average values of all parameters except RHLO, with a 5 % level of significance. The VOR850, DIV200, RHHI, CAPE, MPI, and all oceanic param-
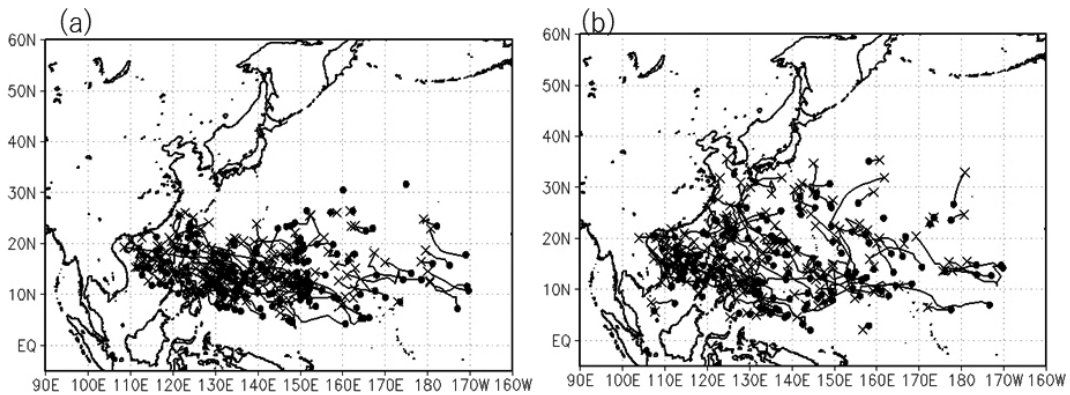
Fig. 2. TC tracks (lines), the first locations (closed circles), and the final locations (crosses) of (a) TSs and (b) TDs between June and October over a 9-year analysis period. The first locations of both TSs and TDs correspond to the first entry of EDA data for each TC. The end location of a TS is the location at which point TS strength was reached. The end location of a TD is the location of the last EDA record for each TC, i.e., when a TD dissipated.
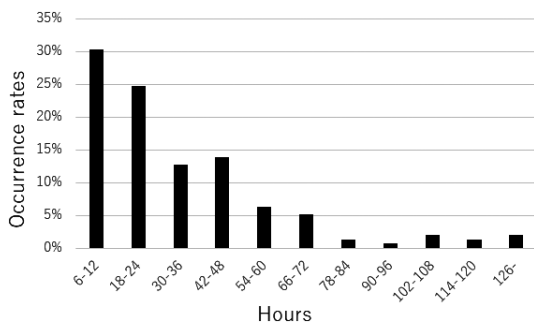

Fig. 3. TD occurrence rate classified into 12-h classes of duration between the first and final records of EDA data for each TD over the 9-year analysis period.

eters of TDs were lower, and the SHRS and SHRD of TDs were higher than those of TSs. Therefore, the large-scale environment around TDs was less favorable for TC development than that around TSs.

3.2 Characteristics of TDs and TSs stratified by environmental factors

Figure 4 presents the TD and TS occurrence distribution stratified by the five environmental factors and UCF. Among the 476 cases, SL was the most frequent factor (155, 33 % of the total), followed by CR (101, 21 %) and EW (80, 17 %). GY (70 TCs) and PTC (44 TCs) were 14 % and 10 %, respectively, and UCF (26 TCs) accounted for 5 %. These percentages were similar to those reported by Yoshida and Ishikawa (2013) using the Joint Typhoon Warning Center best-track data.

The occurrence rates of TDs and TSs stratified by the five environmental factors and UCF are also presented in Fig. 4. The occurrence rate of TDs that formed in environments associated with the CR or PTC was 48 %, which was the lowest among the other factors. Thus, TDs that formed in an environment associated with CR or PTC tended to reach tropical storm strength in their developing stage, resulting in an increase in the number of CR-TSs or PTC-TSs (hereafter, CR-TD, CR-TS, PTC-TD, and PTC-TS; similar terms indicate a TD or a TS that formed in a large-scale flow pattern mainly associated with a CR, PTC, or a similar factor). In contrast, the occurrence rate of EW-TD was 65 %, the highest among the factors. The TDs that formed in an environment associated with EW tended to remain weak in intensity during their developing stage and were therefore less likely to develop into TSs.

In some cases, multiple environmental factors may contribute to TCG. Given that the TGS considered five environmental factors, it is possible to examine not only the main factor but also the factor of the next largest contribution (hereafter secondary factor) (see Appendix A for the definition of the main and secondary factors). Table 4 presents the occurrence numbers and rates of these secondary factors, stratified by the main factors. Secondary-factor occurrence rates are defined as the number of TD or TS secondary factors divided by the number of TD or TS main factors. Interestingly, there were larger differences in the EW secondary-factor occurrence rates between TDs and TSs, specifically differences in the occurrence rates

Table 2. As in Table 1, except the atmospheric environmental physical parameters during the 9-year analysis period between June and October. The CAPE and MPI were computed over 8 years from 2009 to 2016, coinciding with FORA-WNP30.

	ALL		SL		CR		GY	
	TD	TS	TD	TS	TD	TS	TD	TS
VOR850 ($\times 10^{-5}$ s^{-1})	**6.72**	**8.74**	7.95	9.58	**6.16**	**8.64**	8.96	9.59
DIV200 ($\times 10^{-5}$ s^{-1})	**6.23**	**7.39**	6.07	7.19	7.16	7.83	6.27	7.59
RHLO (%)	72	72	73	72	72	73	73	72
RHHI (%)	**48**	**51**	50	51	51	52	48	49
SHRS (m s^{-1})	**4.4**	**3.7**	4.6	3.9	**5.3**	**4.0**	3.5	3.5
SHRD (m s^{-1})	**9.8**	**8.5**	10.0	8.8	**11.0**	**8.8**	10.4	7.9
CAPE (J kg^{-1})	**12694.0**	**13085.4**	12680.0	12839.8	12753.7	13115.0	12675.3	12786.6
MPI (m s^{-1})	**113.9**	**115.7**	113.9	114.5	114.2	115.9	113.8	114.4

	EW		PTC		UCF	
	TD	TS	TD	TS	TD	TS
VOR850 ($\times 10^{-5}$ s^{-1})	4.33	5.81	**4.68**	**9.06**	8.43	9.53
DIV200 ($\times 10^{-5}$ s^{-1})	5.45	5.97	**5.13**	**8.26**	6.81	7.3
RHLO (%)	71	71	71	72	71	72
RHHI (%)	**43**	**48**	**45**	**51**	49	52
SHRS (m s^{-1})	2.8	2.6	4.1	3.8	6.4	4.4
SHRD (m s^{-1})	6.8	7.2	8.4	8.1	13.2	11.4
CAPE (J kg^{-1})	13054.8	13411.3	**12873.0**	**13591.0**	11404.5	12839.9
MPI (m s^{-1})	115.6	117.3	**114.9**	**118.1**	107.6	114.7

Table 3. As in Table 1, except the oceanic physical parameters during the 8-year analysis period from 2009 to 2016 between June and October.

	ALL		SL		CR		GY	
	TD	TS	TD	TS	TD	TS	TD	TS
SST (ºC)	**29.2**	**29.4**	29.3	29.3	29.2	29.4	29.3	29.3
TCHP (kJ cm^{-2})	**98.9**	**116.7**	**95.1**	**113.8**	101.2	113.7	**95.0**	**115.8**
26-°C-depth (m)	**103.1**	**117.3**	**103.0**	**114.4**	101.8	117.2	**93.0**	**117.9**

	EW		PTC		UCF	
	TD	TS	TD	TS	TD	TS
SST (ºC)	29.4	29.5	**29.2**	**29.5**	**28.4**	**29.5**
TCHP (kJ cm^{-2})	110.8	122.7	109.1	126.2	**67.7**	**109.7**
26-°C-depth (m)	113.8	120.1	115.0	121.6	**83.1**	**112.7**

between SL-EW-TD (hereafter main factor–secondary factor) and SL-EW-TS (0.60 vs. 0.45), between CR-EW-TD and CR-EW-TS (0.54 vs. 0.32), and between PTC-EW-TD and PTC-EW-TS (0.67 vs. 0.48). Thus, environments associated with the secondary factor of EW were less favorable for TS development, resulting in an increase (reduction) in the occurrence rates of TDs (TSs). In addition, there were larger differences in the PTC secondary-factor occurrence rates between TDs and TSs, i.e., the occurrence rates between SL-PTC-TD and SL-PTC-TS (0.09 vs. 0.20), between

CR-PTC-TD and CR-PTC-TS (0.13 vs. 0.23), and between GY-PTC-TD and GY-PTC-TS (0.03 vs. 0.16). Therefore, the large-scale environments associated with the secondary factor of PTC were more favorable for TS development, resulting in a reduction (increase) in the occurrence rate of TDs (TSs).

Table 1 also presents the statistical characteristics of TDs and TSs stratified by five environmental factors and UCF; tracks of TDs and TSs are presented in Fig. 5. There were differences in the average location of TCG between TDs and TSs. The CR-TDs, GY-TDs,
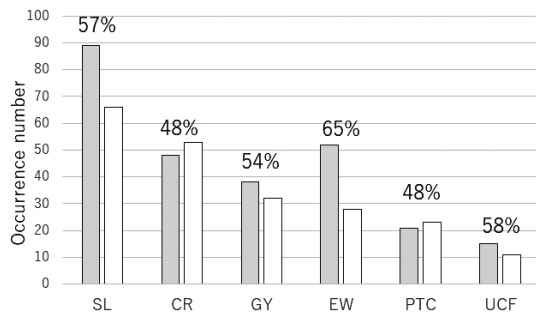
Fig. 4. Distribution of TD and TS occurrence under each environmental factor over the 9-year analysis period. SL: shear line; CR: confluence region; GY: monsoon gyre; EW: easterly waves; PTC: Rossby wave energy dispersion; and UCF: unclassified flow. Gray bars indicate TDs, and white bars indicate TSs. The numbers refer to the occurrence rates of TDs stratified by factors.

and EW-TDs occurred on average farther to the west than did CR-TSs, GY-TSs, and EW-TSs, respectively. In contrast, the average TCG location of PTC-TDs was more biased to the east and north than that of PTC-TSs. As presented in Table 1, there were no differences in the average velocity except for the CR-TD and CR-TS. The average speed of CR-TDs was higher than that of CR-TSs with a 5 % level of significance.

This study compared the average duration of TDs (Table 1) between the first and last entries of EDA data. The average duration of PTC-TDs was 1.93 days, which is approximately 40 % longer than that of all TDs (1.39 days). The average duration of all TSs between the first entry of EDA and the time when tropical storm strength was reached was 1.21 days. The average duration of EW-TSs was 1.66 days, which is approximately 40 % longer than that of all TSs.

3.3 Development conditions of TDs and TSs stratified by environmental factors

Tables 2 and 3 present environmental parameters for TDs and TSs at the time of TCG, stratified by five relevant environmental factors and UCF. There were differences in atmospheric environmental parameters between TD and TS, specifically in the factors of CR, EW, PTC, and UCF. The VOR850 of CR-TDs and PTC-TDs were lower than those of CR-TSs and PTC-TSs, respectively. In addition, the DIV200, RHHI, CAPE, and MPI of PTC-TDs were lower than those of PTC-TSs. The RHHI of EW-TDs was lower than that of EW-TSs. There were no significant differences in SHRS and SHRD, except for the CR; the vertical shear of CR-TDs was significantly higher than that of CR-TSs. It is interesting to note that atmospheric parameters did not differ in SL and GY between TDs and TSs with a 5 % level of significance.

There were differences in the oceanic parameters between TDs and TSs in the factors of SL, GY, PTC, and UCF. The TCHP and the depth of the 26°C isotherm of SL-TDs and GY-TDs were lower than those of SL-TSs and GY-TSs, respectively. The SST of PTC-TDs was lower than that of PTC-TSs. The oceanic parameters did not differ between TDs and TSs for the factors CR and EW with a 5 % level of

Table 4. Occurrence numbers and rates of secondary factors. Secondary-factor occurrence rates were defined as the secondary-factor numbers for TDs or TSs divided by the main-factor numbers for TDs or TSs, respectively.

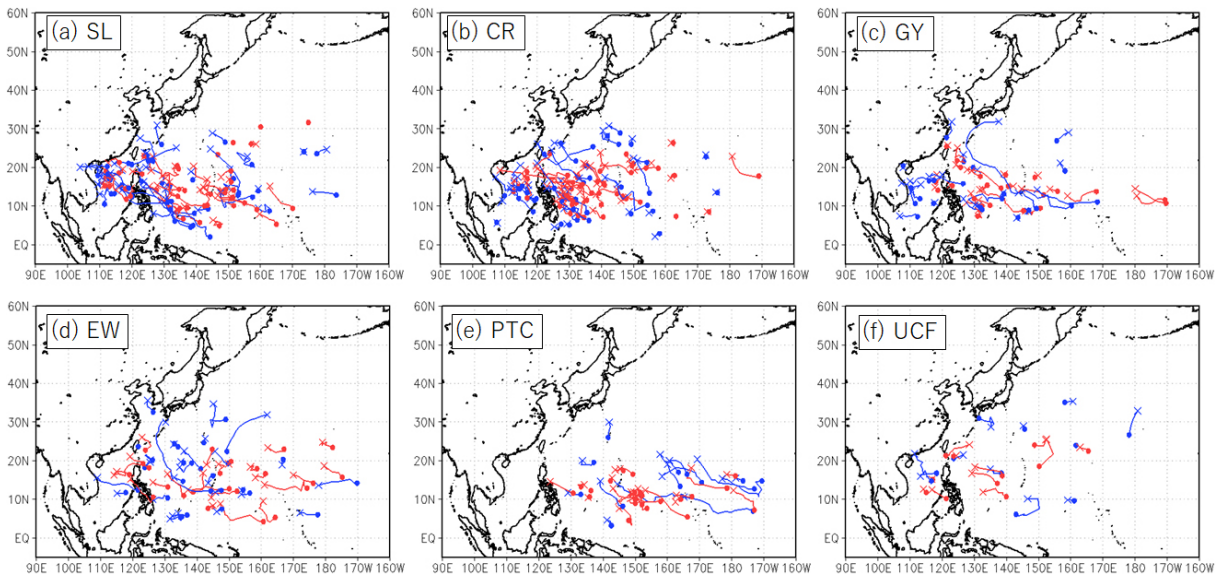| Main factor		Secondary factor									
		SL		CR		GY		EW		PTC	
		TD	TS	TD	TS	TD	TS	TD	TS	TD	TS
SL	Number			13	16	37	29	53	30	8	13
	Rate			0.15	0.24	0.42	0.44	0.60	0.45	0.09	0.20
CR	Number	20	20			12	18	26	17	6	12
	Rate	0.42	0.38			0.25	0.34	0.54	0.32	0.13	0.23
GY	Number	17	13	5	5			24	23	1	5
	Rate	0.45	0.41	0.13	0.16			0.63	0.72	0.03	0.16
EW	Number	0	0	0	0	1	2			0	2
	Rate	0	0	0	0	0.02	0.07			0	0.07
PTC	Number	7	6	3	5	8	5	14	11		
	Rate	0.33	0.26	0.14	0.22	0.38	0.22	0.67	0.48		

Fig. 5.   Same as Fig. 2, except for the tracks of TDs and TSs of (a) SL, (b) CR, (c) GY, (d) EW, (e) PTC, and (f) UCF between June and October over the 9-year analysis period. Blue indicates TD; red indicates TS.
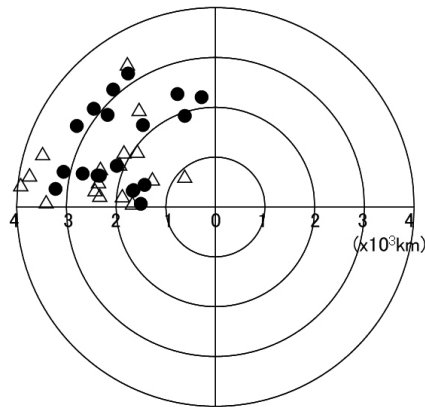

Fig. 6.   Locations of preexisting TCs for PTC-TDs (open triangles) and PTC-TSs (closed circles) relative to the TCG location for each TCG case at the time of TCG over the 9-year analysis period between June and October.
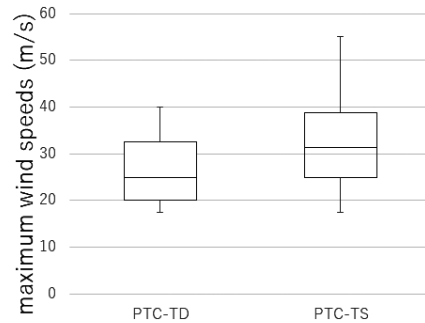

Fig. 7.   Boxplots of maximum sustained wind speeds of preexisting TCs for PTC-TDs and PTC-TSs at the time of TCG over the 9-year analysis period between June and October. The vertical bar indicates the full range of the distribution, and the box indicates the interquartile range of 25–75 % of all cases. The bold horizontal line within each box indicates the median.

significance.

A PTC classified by Ritchie and Holland (1999) is an inherent environmental factor, in that a TC northwest of the TCG location contributes to the TCG of another TC. Figure 6 presents the geographic locations of preexisting TCs, categorized as PTC-TDs and PTC-TSs, with respect to the location of each PTC case at the time of TCG. The average distances between preexisting TCs and TCG locations did not differ significantly, with both averages about 2,800 km. However, the northward average distance of PTC-TDs was significantly shorter than that of PTC-TSs. Interestingly, there was a significant difference between PTC-TDs and PTC-TSs in the intensity of a preexisting TC (Fig. 7); the maximum sustained wind speeds of preexisting TCs were higher for a PTC-TS than for a PTC-TD.

The intense preexisting TC formed the more favorable environment for a development to reach tropical storm strength.

4. Discussion

The environmental factors in which the oceanic environmental parameters of TCHP, including the depth of the 26°C isotherm, significantly differed between TDs and TSs were the SL and GY. The importance of the ocean thermal structure in TC development was recognized by Leipper and Volgenau (1972) and Shay et al. (2000); specifically, SST plays a key role in TCG, but the TCHP plays a more important role in TC intensity changes. Our results therefore suggest that TS developments require higher TCHP values in the lower-tropospheric flow patterns mainly associated with SL or GY. Thus, the development conditions of SL and GY found to be important was higher TCHP. In the other words, an atmosphere–ocean coupled model is needed to improve the TCG prediction associated with SL or GY.

The relevant environmental factors whose atmospheric parameters differed significantly between TDs and TSs were CR, EW, and PTC. The magnitudes of the vertical shear in the mid-lower and upper-lower troposphere were significantly larger in the CR-TD than in the CR-TS. Fudeyasu and Yoshida (2018) focused on TCs with TS intensity or greater in the summer and autumn over the WNP, stratified by the five factors (Ritchie and Holland 1999). Compared with the other factors, the magnitude of vertical shear in the CR was larger at the point in time when tropical storm strength was reached. Despite the differences in the analysis periods used by Fudeyasu and Yoshida (2018), our results clearly showed that CR is associated with intense vertical shear, resulting in an unfavorable environment. Regarding the conditions just prior to reaching TS strength, TSs required a weak vertical shear during their developing stage in environments associated with CR.

The middle-tropospheric relative humidity of EW-TD was significantly lower than that of EW-TS. Dunkerton et al. (2009) showed the center of a closed cyclone circulation (recirculating Kelvin cat's eye) from the TCG cases associated with EW over the North Atlantic and northeastern Pacific Ocean. The Kelvin cat's eye within the critical layer represents a sweet spot for TCG because it provides a containment area for moisture entrained by the developing circulation and/or lofted by the deep convection therein. Numerical simulation studies (e.g., Yoshida et al. 2017) revealed that a TD develops into a TS, with a continuous large-scale environment that contains a large amount of moisture. Our results also revealed that development into a TS associated with EW requires higher-humidity environments.

Both atmospheric and oceanic parameters exhibited a significant difference between TDs and TSs in the PTC and UCF. In addition, an intense preexisting TC formed the more favorable environment for TS development in the PTC (Fig. 7), enhancing the lower-tropospheric relative vorticity (VOR850) and upper-tropospheric divergence (DIV200) (Table 2). Previous studies (e.g., O'Brien and Reid 1967; Leipper 1967; O'Brien 1967; Price 1981) revealed that the passage of a TC induces sea surface cooling, decreasing the sea surface heat flux. Therefore, a preexisting TC in the PTC leads not only to the positive effect of atmospheric environments on TS development but also to the negative effect of the oceanic environment due to sea surface cooling. The developing conditions of PTC-TSs were recognized as higher SST and an intense preexisting TC.

5. Conclusion

This study statistically investigated the characteristics and environmental conditions of TDs over the WNP during the 9 years from 2009 to 2017 that disappeared before reaching tropical storm strength under unfavorable environmental conditions during their developing stage. Using best-track and operational EDA data developed by the JMA, 263 TDs (occurrence rate of 55 %) of 476 cases were detected, based on our definition. The occurrence rate of TD was higher than that of TSs in the winter and spring, whereas the trend was completely the opposite for the period from May to October.

This study also statistically investigated the TD occurrence rates stratified by the environmental factors classified by Ritchie and Holland (1999) using the TGS. The TDs that formed in an environment associated with CR or PTC tended to reach tropical storm strength in their developing stage, resulting in an increase in the number of CR-TSs or PTC-TSs. In contrast, the TDs that formed in an environment associated with EW tended to remain weak in intensity and were therefore less likely to develop into EW-TSs.

The atmospheric and oceanic parameters over the analysis period between June and October differed between TDs and TSs, demonstrating that the large-scale environments around TDs were less favorable for a development than those around TSs. Our results, stratified by five factors and UCF, revealed significant differences in atmospheric (oceanic) parameters be-
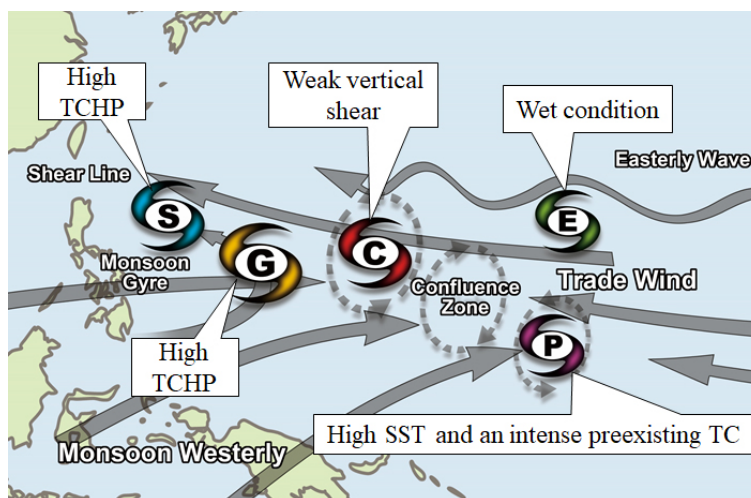
Fig. 8.   Schematic image of the five flow patterns and conditions prior to a TC's reaching TS strength. The westerly and easterly winds are indicated by arrows, and the TCG location (cyclone symbol) of each factor is shown.

tween TDs and TSs in CR, EW, PTC, and UCF (SL, GY, PTC, and UCF). Therefore, the environmental conditions for reaching tropical storm strength during their developing stage, synthesized schematically in Fig. 8, can be summarized as follows: higher TCHP in the SL and GY, weak vertical shear in the CR, wet conditions in the EW, and higher SST and an intense preexisting TC in the PTC.

Differences in the environmental parameter stratified by the lower-tropospheric large-scale flow patterns which contribute to TCG could be considered key determinants of whether a TC develops to tropical storm strength. Thus, the development conditions stratified by environmental factors can be used for operational forecasting. Our results also indicate that an atmosphere–ocean coupled model is needed to improve the TCG prediction skills as well as to the TC intensity prediction skills.

Appendix A

The TGS developed by Yoshida and Ishikawa (2013) was used in this study. To describe the contributions from the five flow patterns to each TCG case, we first compute five scores, SCR_{SL}, SCR_{CR}, SCR_{GY}, SCR_{EW}, and SCR_{PTC}, using the following equations:

$$SCR_{SL} = A\left(\frac{\partial u}{\partial y}\right)_{ave} \cdot \exp(B \cdot dist), \tag{1}$$

$$SCR_{CR} = A\left(\frac{\partial u}{\partial x}\right)_{ave} \cdot \exp(B \cdot dist), \tag{2}$$

$$SCR_{EW} = A\left(\frac{\partial v}{\partial x}\right)_{ave} \cdot \exp(B \cdot dist), \tag{3}$$

$$SCR_{GY} = \exp(-M) \times (\zeta - \zeta_{std}), \tag{4}$$

$$SCR_{PTC} = C_{wv1}^2, \tag{5}$$

where u and v indicate the zonal and meridional winds at the 850 hPa level, $dist$ indicates the distance from the location of TCG, and ζ indicates the relative vorticity which is expressed as the excess above the standard value $\zeta_{std} = -1.0 \times 10^{-5}$ s^{-1}. A and B are arbitrary constants with $A = -1.0$ (2.0×10^{-1}) and $B = -1.0 \times 10^{-5}$ (-1.0×10^{-2}) for SCR_{SL} and SCR_{CR}

(SCR_{EW}). For SCR_{GY}, $M = \sum_{i=0}^{ni} \sum_{j=0}^{nj} \sqrt{(C'_{(i,j)} - data'_{(i,j)})^2}$ is computed where C' indicates the sea-level pressure field to a composite of typical GY cases reported by Lander (1994), $data'$ indicates the sea-level pressure field of a TCG case, i and j indicate the horizontal grid, and ni and nj indicate the width and length, respectively. For SCR_{PTC}, we compute the amplitude of the first Fourier-component C^2_{wv1} of sea-level pressure along the line connecting the preexisting TC and TCG locations. An upper limit of 1,500 km is set for the $dist$, and a lower limit of 1.01 is set for C^2_{wv1}. After each score is normalized by its maximum and minimum values, the flow pattern with the highest score is determined to be the main factor. The flow pattern of the next largest score is determined to be the secondary factor. Details of the TGS are illustrated by Yoshida and Ishikawa (2013) and Fudeyasu and Yoshida (2018, 2019).

References

Bister, M., and K. A. Emanuel, 1998: Dissipative heating and hurricane intensity. *Meteor. Atmos. Phys.*, **65**, 233–240.

Blake, E., and S. D. Kotal, 2018: Cyclogenesis: Operational forecasting perspectives. *Sub-topic report at the 9th WMO International Workshop on Tropical Cyclones*, 28 pp.

Dunkerton, T. J., M. T. Montgomery, and Z. Wang, 2009: Tropical cyclogenesis in a tropical wave critical layer: easterly waves. *Atmos. Chem. Phys.*, **9**, 5587–5646.

Dvorak, V. F., 1984: *Tropical Cyclone Intensity Analysis Using Satellite Data*. NOAA Tech. Rep. NESDIS 11, 47 pp.

Emanuel, K. A., 1986: An air-sea interaction theory for tropical cyclones. Part I: Steady-state maintenance. *J. Atmos. Sci.*, **43**, 585−604.

Fu, B., M. S. Peng, T. Li, and D. E. Stevens, 2012: Developing versus nondeveloping disturbances for tropical cyclone formation. Part II: Western North Pacific. *Mon. Wea. Rev.*, **140**, 1067–1080.

Fudeyasu, H., and R. Yoshida, 2018: Western North Pacific tropical cyclone characteristics stratified by genesis environment. *Mon. Wea. Rev.*, **146**, 435–446.

Fudeyasu, H., and R. Yoshida, 2019: Statistical analysis of the relationship between upper tropospheric cold lows and tropical cyclone genesis over the western North Pacific. *J. Meteor. Soc. Japan*, **97**, 439–451.

Gray, W. M., 1968: Global view of the origin of tropical disturbances and storms. *Mon. Wea. Rev.*, **96**, 669–700.

Gray, W. M., 1998: The formation of tropical cyclones. *Meteor. Atmos. Phys.*, **67**, 37–69.

Halperin, D. J., H. E. Fuelberg, R. E. Hart, J. H. Cossuth, P. Sura, and R. J. Pasch, 2013: An evaluation of tropical cyclone genesis forecasts from global numerical models. *Wea. Forecasting*, **28**, 1423–1445.

Halperin, D. J., R. E. Hart, and H. E. Fuelberg, 2017: The development and evaluation of a statistical–dynamical tropical cyclone genesis guidance tool. *Wea. Forecasting*, **32**, 27–46.

Kishimoto, K., 2008: *Revision of JMA's early stage Dvorak analysis and its use to analyze tropical cyclones in the early developing stage*. RSMC Tokyo—Typhoon Center Technical Review, **10**, 1–12. [Available at http://www.jma.go.jp/jma/jma-eng/jma-center/rsmc-hp-pub-eg/techrev/text10-1.pdf.]

Kishimoto, K., T. Nishigaki, S. Nishimura, and Y. Terasaka, 2007: *Comparative study on organized convective cloud systems detected through early stage Dvorak analysis and tropical cyclones in early developing stage in the western North Pacific and the South China Sea*. RSMC Tokyo—Typhoon Center Tech. Review, **9**, 14 pp. [Available at http://www.jma.go.jp/jma/jma-eng/jma-center/rsmc-hp-pub-eg/techrev/text9-2.pdf.]

Knaff, J. A., C. R. Sampson, and M. DeMaria, 2005: An operational statistical typhoon intensity prediction scheme for the western North Pacific. *Wea. Forecasting*, **20**, 688–699.

Koba, H., T. Hagiwara, S. Asano, and S. Akashi, 1990: Relationships between CI number from Dvorak's technique and minimum sea-level pressure or maximum wind speed of tropical cyclone. *J. Meteor. Res.*, **42**, 59–67 (in Japanese).

Kobayashi, S., Y. Ota, Y. Harada, A. Ebita, M. Moriya, H. Onoda, K. Onogi, H. Kamahori, C. Kobayashi, H. Endo, K. Miyaoka, and K. Takahashi, 2015: The JRA-55 Reanalysis: General specifications and basic characteristics. *J. Meteor. Soc. Japan*, **93**, 5–48.

Lander, M. A., 1994: Description of a monsoon gyre and its effects on the tropical cyclones in the western North Pacific during August 1991. *Wea. Forecasting*, **9**, 640–654.

Leipper, D. F., 1967: Observed ocean conditions and Hurricane Hilda, 1964. *J. Atmos. Sci.*, **24**, 182–196.

Leipper, D. F., and D. Volgenau D, 1972: Hurricane heat potential of the Gulf of Mexico. *J. Phys. Oceanogr.*, **2**, 218–224.

O'Brien, J. J., 1967: The non-linear response of a two-layer, baroclinic ocean to a stationary, axially-symmetric hurricane: Part II. Upwelling and mixing induced by momentum transfer. *J. Atmos. Sci.*, **24**, 208–215.

O'Brien, J. J., and R. O. Reid, 1967: The non-linear response of a two-layer, baroclinic ocean to a stationary, axially-symmetric hurricane: Part I. Upwelling induced by momentum transfer. *J. Atmos. Sci.*, **24**, 197–207.

Peng, M. S., B. Fu, T. Li, and D. E. Stevens, 2012: Developing versus nondeveloping disturbances for tropical cyclone formation. Part I: North Atlantic. *Mon. Wea. Rev.*, **140**, 1047–1066.

Price, J. F., 1981: Upper ocean response to a hurricane. *J.*

Phys. Oceanogr., **11**, 153–175.

Ritchie, E. A., and G. J. Holland, 1999: Large-scale patterns associated with tropical cyclogenesis in the western Pacific. *Mon. Wea. Rev.*, **127**, 2027–2043.

Shay, L. K., G. J. Goni, and P. G. Black, 2000: Effects of a warm oceanic feature on Hurricane Opal. *Mon. Wea. Rev.*, **128**, 1366–1383.

Tsuchiya, A., T. Mikawa, and A. Kikuchi, 2001: Method of distinguishing between early stage cloud systems that develop into tropical storms and ones that do not. *Geophys. Mag.*, **4**, 49–59.

Usui, N., T. Wakamatsu, Y. Tanaka, N. Hirose, T. Toyoda, S. Nishikawa, Y. Fujii, Y. Takatsuki, H. Igarashi, H. Nishikawa, Y. Ishikawa, T. Kuragano, and M. Kamachi, 2017: Four-dimensional variational ocean reanalysis: A 30-year high-resolution dataset in the western North Pacific (FORA-WNP30). *J. Oceanogr.*, **73**, 205–233.

Wada, A., 2015: Verification of tropical cyclone heat potential for tropical cyclone intensity forecasting in the western North Pacific. *J. Oceanogr.*, **71**, 373–387.

Yamaguchi, M., and N. Koide, 2017: Tropical cyclone genesis guidance using the early stage Dvorak analysis and global ensembles. *Wea. Forecasting*, **32**, 2133–2141.

Yamaguchi, M., F. Vitart, S. T. K. Lang, L. Magnusson, R. L. Elsberry, G. Elliott, M. Kyouda, and T. Nakazawa, 2015: Global distribution of the skill of tropical cyclone activity forecasts on short- to medium-range time scales. *Wea. Forecasting*, **30**, 1695–1709.

Yamaguchi, M., H. Titley, and L. Magnusson, 2018: Current and potential use of ensemble forecasts in operational TC forecasting. *Sub-topic report at the 9th WMO International Workshop on Tropical Cyclones*, 28 pp.

Yoshida, R., and H. Ishikawa, 2013: Environmental factors contributing to tropical cyclone genesis over the western North Pacific. *Mon. Wea. Rev.*, **141**, 451–467.

Yoshida, R., Y. Miyamoto, H. Tomita, and Y. Kajikawa, 2017: The effect of water vapor on tropical cyclone genesis: A numerical experiment of a non-developing disturbance observed in PALAU2010. *J. Meteor. Soc. Japan*, **95**, 35–47.

Zhang, W., B. Fu, M. S. Peng, and T. Li, 2015: Discriminating developing versus nondeveloping tropical disturbances in the western North Pacific through decision tree analysis. *Wea. Forecasting*, **30**, 446–454.

Zehr, R. M., 1992: *Tropical cyclogenesis in the western North Pacific*. NOAA Tech. Rep. NESDIS 61, 181 pp.